Science Robotics

robotics.sciencemag.org/cgi/content/full/3/17/eaas8713/DC1

Supplementary Materials for

Geometric constraints and optimization in externally driven propulsion

Yoni Mirzae, Oles Dubrovski, Oded Kenneth, Konstantin I. Morozov, Alexander M. Leshansky*

*Corresponding author. Email: lisha@technion.ac.il

Published 18 April 2018, *Sci. Robot.* **3**, eaas8713 (2018)
DOI: 10.1126/scirobotics.aas8713

This PDF file includes:

Supplementary Materials

Shape and magnetization of some optimal propellers

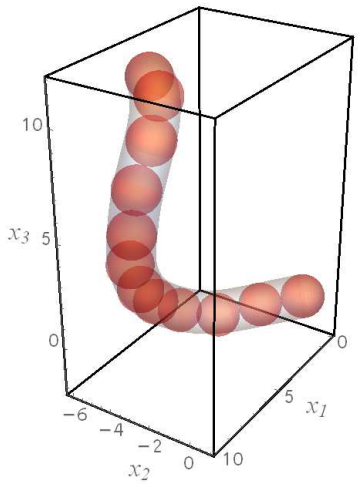

Fig. S1. δ-optimal propeller (Fig. 3). The drawing of the bead-based δ-optimal propeller tabulated in Table S1 together with the approximate smooth envelope.

x_1	x_2	x_3
1.00	0.00	0.00
1.892	-1.702	-0.555
2.945	-3.308	-1.113
4.469	-4.404	-0.425
6.058	-4.588	0.776
7.455	-4.334	2.184
8.427	-4.098	3.916
9.030	-3.507	5.729
8.925	-3.280	7.714
8.086	-3.120	9.522
6.634	-3.767	10.736
5.254	-5.212	10.830

Table S1. Tabulated shape of the δ-optimal propeller (Fig. 3). Coordinates of the beads (with radius $a = 1$) composing the δ-optimal propeller with aspect ratio 1:12 as obtained using unconstrained optimal search.

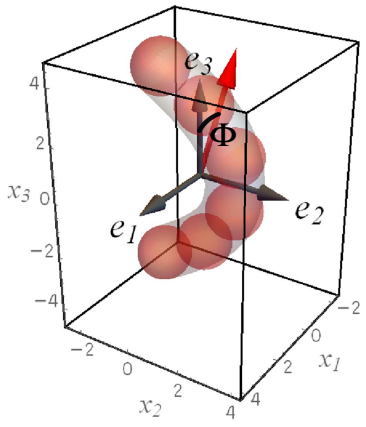

Fig. S2. δ^*-optimal propeller (Fig. 4A). The drawing of the δ^*-optimal propeller tabulated in Table S2. $\{\boldsymbol{e}_1, \boldsymbol{e}_2, \boldsymbol{e}_3\}$ stand for the principal rotation axes; the optimal magnetization (red arrow) angles are $\alpha = \pi$ and $\Phi = 0.535$.

x_1	x_2	x_3
0.	-1.557	-3.596
0.	0.170	-2.586
0.	1.387	-1.00
0.	1.387	1.00
0.	0.170	2.586
0.	-1.557	3.596

Table S2. Tabulated shape of the δ^*-optimal propeller (Fig. 4A). Coordinates of the beads (with radius $a = 1$) composing the δ^*-optimal propeller with two-fold reflection symmetry. The coordinate frame is aligned with principal rotation axes.

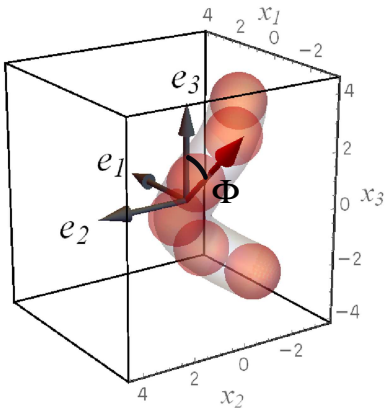

Fig. S3. δ^*-optimal propeller (Fig. 4B). The drawing of the δ^*-optimal propeller tabulated in Table S3; $\{\boldsymbol{e}_1, \boldsymbol{e}_2, \boldsymbol{e}_3\}$ stand for the principal rotation axes; the optimal magnetization (red arrow) angles are $\alpha = \pi$ and $\Phi = 0.803$.

x_1	x_2	x_3
-0.499	-2.516	-3.009
0.911	-1.282	-2.311
0.586	0.00	-0.810
-0.586	0.00	0.810
-0.911	-1.282	2.311
0.499	-2.516	3.009

Table S3. Tabulated shape of the δ^*-optimal propeller (Fig. 4B). Coordinates of the beads (with radius $a = 1$) composing the δ^*-optimal skew-symmetric propeller. The coordinate frame is aligned with principal rotation axes.

Overall best δ^*-optimal propeller (Fig. 6)

The tabulated (bead-based) shape of the overall best δ^*-optimal propeller that we use to compute the velocity-frequency dependence for different orientation of the magnetic moment $\boldsymbol{m}$ is provided in Table S4. The size of the propeller (i.e., the diameter of the smallest ball that fully encircles the propeller) is $\ell = 6.44\,a$ with a being the radius of a bead. The corresponding rotational mobility of the propeller in the frame of *principal axes of rotation* has the diagonal form

$$\boldsymbol{\mathcal{F}} = \frac{10^{-3}}{\eta a^3}\,\mathrm{diag}(3.13,\,3.33,\,7.42)\,,$$

where η stands for viscosity of the suspending fluid. The corresponding chirality matrix (i.e., symmetrized $\boldsymbol{\mathcal{G}} \cdot (\boldsymbol{\mathcal{F}}\ell)^{-1}$) reads

$$\mathbf{Ch} = \begin{pmatrix} 0.00287 & 0. & 0.0112 \\ 0. & -0.00601 & 0. \\ 0.0112 & 0. & 0.00340 \end{pmatrix}\,.$$

The magnetization angles maximizing (i) δ^* are $\alpha = \pi$, $\Phi = 0.67$ (solid red line in Fig. 6); (ii) δ at the step-out: $\alpha = \pi$, $\Phi = 0.41$ (dashed blue line); (iii) δ at intermediate frequencies: $\alpha = -1.75$, $\Phi = 1.17$ (solid green line), $\alpha = -1.96$, $\Phi = 0.85$ (solid cyan line) and $\alpha = -2.25$, $\Phi = 0.60$ (solid magenta line); (iv) for transverse magnetization: $\Phi = \pi/2$ and arbitrary value of α (dotted line);

x_1	x_2	x_3
0.102	-1.440	2.220
-0.389	0.000	0.921
0.389	0.000	-0.921
-0.102	-1.440	-2.220

Table S4. Tabulated shape of δ^*-optimal propeller (Fig. 6). Coordinates of the beads (with radius $a = 1$) composing the δ^*-optimal skew-symmetric propeller with aspect ratio 1:4 used to compute velocity-frequency curves in Fig. 6 in the main text. The coordinate frame is aligned with principal rotation axes $\{\boldsymbol{e}_1, \boldsymbol{e}_2, \boldsymbol{e}_3\}$.

The effect of magnetization on propulsion of random aggregate

To demonstrate the effect of magnetization on propulsion of the random clusters we take a representative random aggregate shown in Fig. S4. The propulsion efficiency of this aggregate $\delta_{\max} \approx 0.061$ is about the same as the average value of $\delta_{\max}$ (see Fig. 2C in the main text).

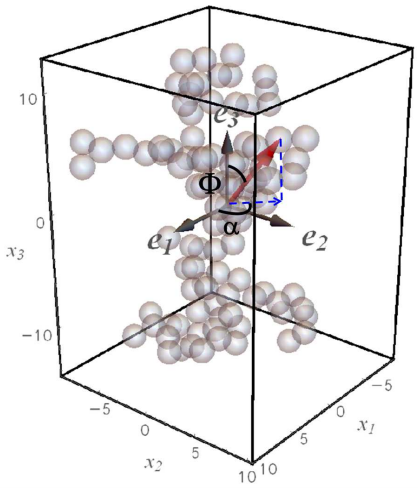

Fig. S4. Typical random aggregate. Representative random aggregate made of 100 beads (of radius $a = 1$) with $D_f = 2$ and $k_f = 1.2$; the size of the aggregate is $\ell = 26.97\,a$. The shown reference frame is aligned with principal axes of rotation $\{\boldsymbol{e}_1, \boldsymbol{e}_2, \boldsymbol{e}_3\}$ and magnetization orientation (red arrow, $\alpha = 2.013$, $\Phi = 0.598$) corresponds to the maximum propulsion velocity $U_{Z,\max}$ (at the step-out).

We further plot the ratio $|U_Z/U_{Z,\max}|$ upon varying the orientation of the magnetic moment $\boldsymbol{m}$ (via the angles α and Φ) affixed to this aggregate (see Fig. S5). It can be readily seen that magnetization orientation is critical for efficient propulsion, as for arbitrary magnetization U_Z is significantly below $U_{Z,\max}$. For the optimal orientation of $\boldsymbol{m}$ shown in Fig. S4 we find $\delta^*_{\max} = 0.27{\cdot}10^{-5}$, which is about two orders-of-magnitude lower than the corresponding values found for δ^*-optimal propellers (see Table 2). Moreover, in the experiments the magnetization cannot be controlled and as a result much lower values of δ^* are expected as illustrated in Fig. S5.

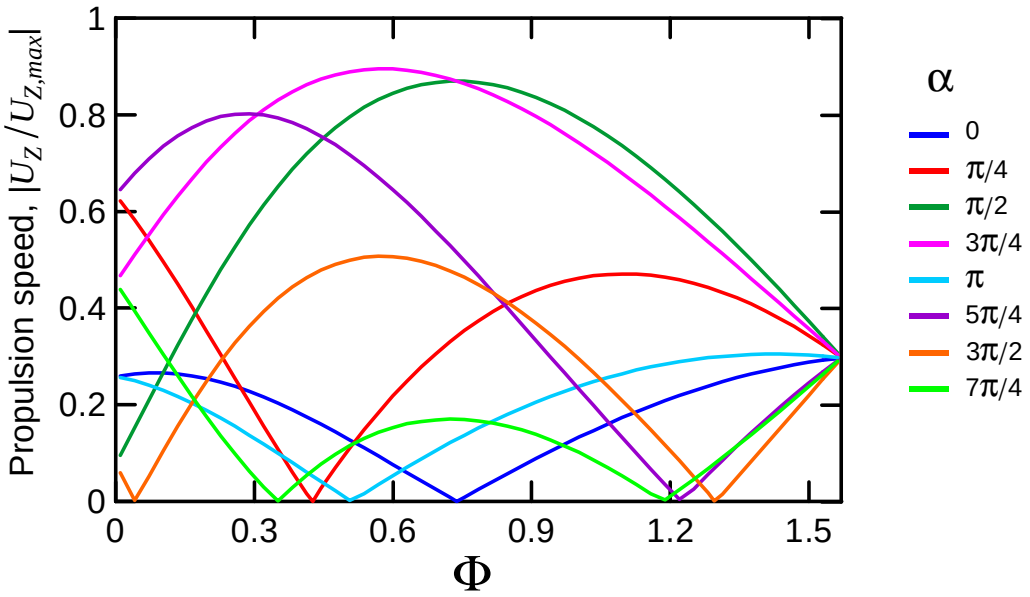

Fig. S5. Effect of magnetization on propulsion of a random aggregate. The scaled propulsion velocity $|U_Z/U_{Z,\max}|$ of the aggregate in Fig. S4 vs. the polar magnetization angle Φ. Different curves correspond to different values of the azimuthal magnetization angle α. The optimal magnetization corresponding to $|U_Z/U_{Z,\max}| = 1$ is attained at $\alpha = 2.013$, $\Phi = 0.598$.